

Stochastic activations

Maria Lomeli¹, Matthijs Douze¹, Gergely Szilvasy¹, Loic Cabannes^{1,2,3}, Jade Copet¹, Sainbayar Sukhbaatar¹, Jason Weston¹, Gabriel Synnaeve¹, Pierre-Emmanuel Mazaré¹, Hervé Jégou¹

¹Meta FAIR, ²Ecole Normale Supérieure Paris Saclay, ³Paris Cité University

We introduce stochastic activations. This novel strategy randomly selects between several non-linear functions in the feed-forward layer of a large language model. In particular, we choose between `SILU` or `RELU` depending on a Bernoulli draw. This strategy circumvents the optimization problem associated with `RELU`, namely, the constant shape for negative inputs that prevents the gradient flow. We leverage this strategy in two ways:

(1) We use stochastic activations during pre-training and fine-tune the model with `RELU`, which is used at inference time to provide sparse latent vectors. This reduces the inference FLOPs and translates into a significant speedup in the CPU. Interestingly, this leads to much better results than training from scratch with the `RELU` activation function.

We evaluate stochastic activations for sequence generation. This strategy performs reasonably well: it has higher diversity and is only slightly inferior in terms of performance to the best deterministic non-linearity, namely, `SILU` combined with temperature sampling. This offers an alternative to existing strategies by providing a controlled way to increase the diversity of the generated text.

Date: December 23th 2025

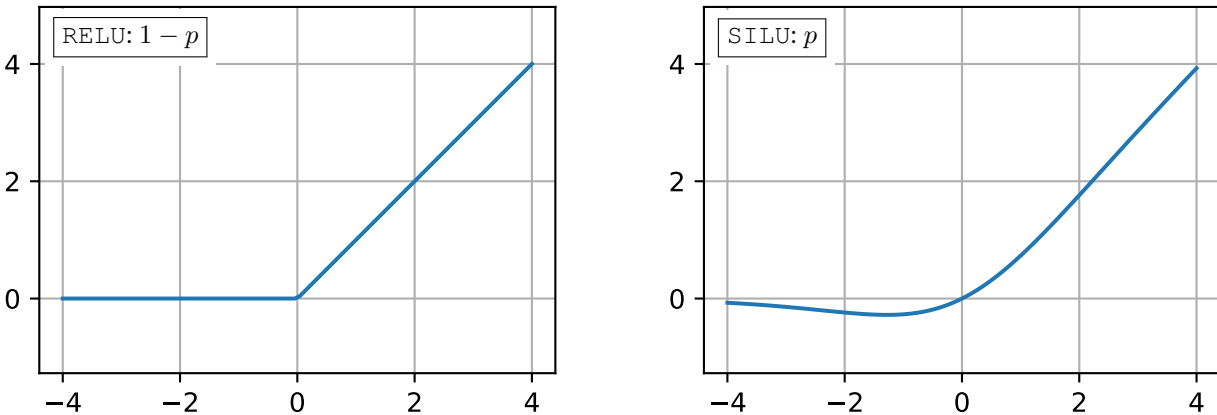


Figure 1 Stochastic activation randomly selects one of two activations when $x < 0$:

(1) `RELU` selected with probability $1 - p$; otherwise (2) another activation, in particular `SILU`.

1 Introduction

Large language models (LLMs) (Devlin et al., 2019; Chowdhery et al., 2022; Brown et al., 2020; Vaswani et al., 2017) have revolutionized natural language processing, enabling unprecedented capabilities in text generation, comprehension, and reasoning. Their success stems from scaling model parameters and leveraging vast amounts of data, but this comes with a significant computational complexity. As the demand for

more efficient and powerful models grows, researchers are increasingly focused on optimizing their training processes to balance performance with resource constraints.

The majority of the LLM parameters are in the Feed-Forward Network (FFN) layers, where they primarily serve to store and recall information from the training data. FFNs are two linear layers separated by an *activation function*, and sometimes an additional linear layer that serves as a gating operation. The activation is a non-linear function from \mathbb{R} to \mathbb{R} . In this context, the choice of activation function plays a crucial role for both the model’s expressivity and efficiency. The simplest choice of activation is RELU (Rectified Linear Unit), that allows positive values to pass through and forces negative inputs to zero. RELU is *sparsity-inducing*, since, on average, half of its outputs are zero (in practice significantly more). Within a two-layer Multilayer Perceptron, this means that inference on the second layer is a matrix-sparse vector multiplication, hence, it can be implemented with fewer FLOPs than a matrix-dense vector multiplication. Note that effectively improving the runtime with this sparsity pattern remains challenging.

In practice, the Sigmoid Linear Unit (SILU) activation, combined with a gated design, has consistently outperformed RELU in terms of model accuracy (Shazeer, 2020). Unfortunately, SILU does not induce sparsity. One plausible explanation for RELU’s underperformance is that its gradient for negative input values is zero, which hinders optimization by preventing weight updates in a significant portion of the network. Solutions like Leaky RELU (Maas et al., 2013) circumvent this problem by ensuring non-zero gradient almost everywhere, but they are inferior to SILU and involve abandoning sparsity. In contrast, if the so-called “dying RELU problem” optimization challenge could be effectively addressed, RELU’s theoretical advantages – such as sparsity and computational efficiency – may translate into performance comparable to SILU for a lower number of FLOPs. This disparity presents a challenge: how to harness the efficiency benefits of sparse activations, such as RELU, without sacrificing the empirical advantages of SILU. This motivates our exploration of alternative training strategies that mitigate RELU’s limitations while preserving its benefits.

In this work, we consider two ways to approach this problem. The first approach is activation fine-tuning, denoted by S_{wi+FT} : we pre-train the model with an activation that facilitates efficient large language model optimization, then, we change the activation to RELU and adapt the model by fine-tuning it further. Our second approach, referred to as S_{tochA} (stochastic activations), is a novel technique that randomly selects between multiple activations, either at train or test time. Both approaches allow models to benefit from the superior optimization properties of SILU. These hybrid strategies combine the best of both worlds – maintaining high model performance while unlocking the computational efficiency of sparse activations.

In summary, this paper makes the following contributions:

- We introduce two strategies that employ different activation functions at training and inference time, namely S_{wi+FT} and S_{tochA} . Both are complementary and make it possible to use activations at inference time that differ from those employed during pre-training.
- We produce RELU-based models that are much better than those obtained with regular training, i.e., our methods significantly outperform training with RELU only.
- We show that stochastic activations, when used at inference time, provide an alternative way to generate diverse sequences compared to traditional temperature sampling or other variants.

2 Related work

Standard activation functions Activations are at the core of deep learning, they are fundamental to enable deep learning models to go beyond linear function with limited expressivity. While early neural network architectures were inspired by logistic regression, such as sigmoidal and tanh activations, many activation functions have been evaluated for the FFN layers of transformers. Vaswani et al. (2017) used RELU (Glorot et al., 2011) initially. However, using the RELU activation function leads to some neurons getting stuck in the negative region. As a consequence, models stop learning entirely, since the gradient is zero for negative inputs, and their weights do not get updated. In contrast, Touvron et al. (2023) used SILU as the activation function for the FFN layers of the transformer for the first Llama models. Shazeer (2020) discusses the benefits of SWIGLU, which consists of SILU with gating. There exist many other activation functions such

as the Gaussian Error Linear Unit (GELU) (Hendrycks & Gimpel, 2016), Scaled Exponential Linear Unit (SELU) (Klambauer et al., 2017), Swish (Ramachandran et al., 2018) and gated SiLU, among others.

In particular, the Leaky RELU (Maas et al., 2013; Redmon et al., 2015; Ridnik et al., 2021; Guo et al., 2024) tried tackling the dying RELU problem by allowing a small, non-zero gradient when the input is negative in order to keep the neurons active and the gradients flowing, reducing the risk of dead neurons.

Adaptive activation functions Lee et al. (2022) propose the Adaptive Swish (ASH) activation, which uses stochastic sampling of the top-k percentile elements. It generalizes the Swish (Ramachandran et al., 2018), which uses adaptive thresholding to select the values in the top percentiles and is set to zero otherwise. It is an example of a stochastic activation.

Dropout and structured Dropout variants In the original dropout paper (Srivastava et al., 2014), the authors propose a regularization technique to reduce overfitting and improve generalization of a neural network. It consists of setting to zero a subset of neurons at each training step. Consequently, the dropped neurons do not contribute to the forward pass or receive weight updates during back-propagation. At inference time, all neurons are used and their outputs are scaled by the dropout probability.

LayerDrop (Fan et al., 2019) randomly drops entire layers during training, hence, it encourages the model to be robust to missing layers. At inference time, some layers can be pruned, trading off speed and accuracy as needed. While the method does not make the model sparse in the usual sense, it induces structured sparsity in the computation graph during training. Other works also introduce structured dropout variants such as DropBlock (Ghiasi et al., 2018), Bayesian dropout (Gal & Ghahramani, 2016), or Beit (Bao et al., 2021) and masked-autoencoder (He et al., 2022) in computer vision, among others.

Quantization approaches Fan et al. (2020) propose Quant-noise, that mimicks quantization during training by introducing noise to a random subset of weights for each forward pass enabling high compression ratios while maintaining the original model performance. It uses the Straight-Through estimator (STE) (Bengio et al., 2013; Hinton, 2012) to compute the gradients. This training technique ensures that the model is pretrained to observe both the train-time (unquantized) and the inference-time (quantized) models. This ensures proper optimization, bypassing the flat gradient caused by quantization and reducing the discrepancy that results from the late quantization of the model weights.

Sparsity by design Some works propose to enable sparsity directly in the architecture, for instance, the Mixture of Experts (MoE) or the Product-Key Memory (PKM). The PKM architecture (Lample et al., 2019) uses a memory layer for neural networks which enables the model to access a large learnable memory and thus, it enables long term memory capabilities. It leverages product quantization (PQ) (Jégou et al., 2011) by splitting the key in two parts and using each part in separate codebooks. The combination of each PQ index enables the model to access a larger memory space efficiently. At each forward pass, only a small subset of the memory is accessed, making it computationally efficient.

Mixture of Expert (MoE) models (Yang et al., 2024; Wei et al., 2024; DeepSeek-AI et al., 2024; Jiang et al., 2024) dynamically select and activate the relevant subset of parameters based on the characteristics of the input data. The MoE approach allows MoE models to expand their capacity without proportionally increasing computational complexity. See Mu & Lin (2025) for an overview of the MoE and references therein.

3 Using different activations at train and test time

This section introduces two strategies for improving the optimization during pretraining using an optimization-compliant activation, while preparing the model to a potentially different activation at test time. First we introduce the Swi+FT fine-tuning approach. Then we introduce our Stochastic Activation StochA.

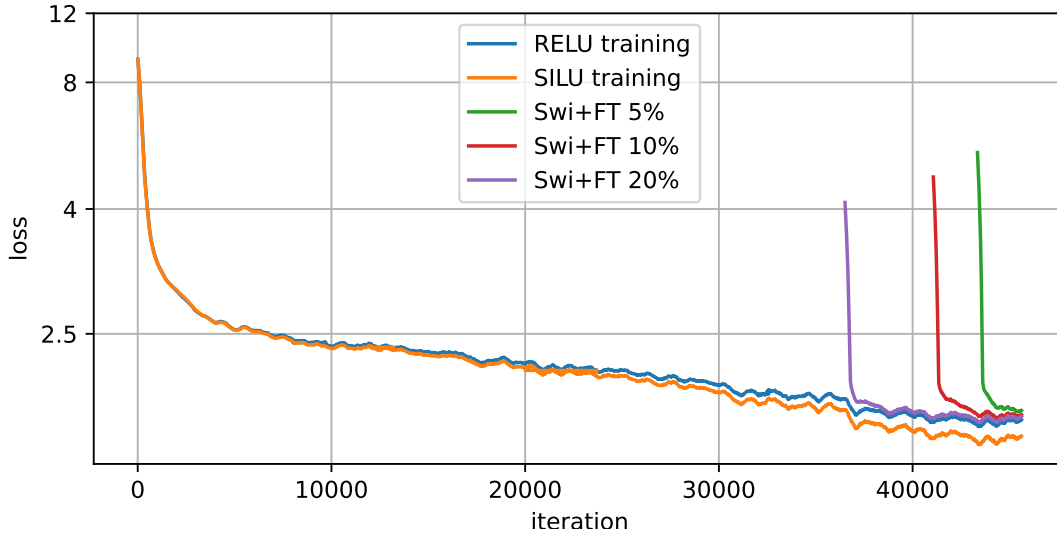


Figure 2 Swi+FT: Training loss. Most of the training is carried out with `SILU`, with $\alpha * 100\% = 5\%$, 10% and 20% of the final steps using `RELU`. Note the loss spike when we switch the activation. The model rapidly recovers and converges to a regime where `RELU` is performing well while providing sparsity.

3.1 Fine-tuning with `RELU`: Swi+FT

In the following, we use `SILU` and `RELU` as our training and inference activations. For reference, they are defined in $\mathbb{R} \rightarrow \mathbb{R}$ as:

$$\text{RELU}(x) = \max(x, 0) \quad \text{SILU}(x) = x\sigma(x), \quad (1)$$

where $\sigma(x) = 1/(1 + \exp(-x))$ is the sigmoid function. We choose these two activations because `SILU` is one of the best options in terms of accuracy, while `RELU` is simple and sparse. The two activations are also similar: same asymptotes at $-\infty$ and $+\infty$, and the same value at 0. `SILU` is differentiable twice (unlike `RELU`) and, interestingly, non-monotonous.

In our proposed approach, the training operates as follows:

- Most of the training steps (during a proportion $1 - \alpha$ of the total number of iterations) are carried out with a first activation that is deemed preferable for training. We typically employ `SILU` for this stage.
- We then switch the activation to that used for inference for the rest of the training.

We mostly set $\alpha = 0.05$ or $\alpha = 0.1$, which mean that only 5% or 10% of the training steps are carried out using the inference-time activation. We do not re-initialize the parameters of the optimizer when switching between activations, and similarly we do not use any warm-up. This does not disrupt the optimization because the `SILU` and `RELU` activations are relatively similar. We observe a spike in the loss at the time we change the activation, see Figure 2. However, the optimization rapidly recovers. In practice, the fine-tuning replaces the last iterations of the pretraining. The learning rate follows a cosine schedule which gradually reduces it to $1/100^{\text{th}}$ of its peak value. Therefore, at 5% or 10% of the end of the training, the learning rate is already $60\times$ or $29\times$ lower than its peak, which is compatible with a fine-tuning regime.

3.2 Stochastic activation: StochA

A stochastic function, parametrized by a random variable ω , is a function

$$y = \Psi(x, \omega) \quad (2)$$

that maps inputs $x \in \mathbb{R}$ to output $y \in \mathbb{R}$ with randomness involved. The dependence on ω emphasizes that the outcome depends on an underlying probability space. In that sense, the function $\Psi(\cdot, \omega)$ is deterministic

for each realization of ω , but is stochastic overall. In particular, we consider the case depicted in Figure 1, where $\omega \sim \text{Bernoulli}(p)$ is a binary random variable parametrized by a parameter $p: \omega \in \{0, 1\}$ such that $\mathbb{P}(\omega = 1) = p$ and $\mathbb{P}(\omega = 0) = 1 - p$. In that case, the stochastic function $\Psi_p(\cdot)$ is defined such that

$$\text{if } x < 0, \Psi_p(x) = (1 - \omega) \times \text{RELU}(x) + \omega \times \text{SILU}(x), \quad (3)$$

which corresponds to randomly selecting between the `RELU` and `SILU` activations for $x < 0$. If $x \geq 0$ we choose $\Psi_p(x) = x$ or $\Psi_p(x) = \text{SILU}(x)$, see the baselines description below.

This strategy ensures that the network is compatible with two regimes. The first one, drawn with probability $1 - p$, is the inference-time mode, where we prepare the network to employ `RELU` during generation, in order to exhibit sparsity. The second mode aims to facilitate optimization during training. The choice of the `SILU` activation is motivated by the regular deterministic gated design by (Shazeer, 2020) adopted by most state-of-the-art LLMs.

Notation To specify an activation, we separately define the function for the positive and negative range of inputs. For example `R-S+` means that `RELU` is used for the negative range and `SILU` for the positive. When `StochA` is used, we indicate `[S|R]-S+`, which means that for the negative range, we sample `SILU` with probability p and `RELU` with probability $1 - p$.

Baselines The two natural baselines are the deterministic functions `SILU` and `RELU`. We also introduce two non-stochastic baselines in order to disentangle the effect that could come from combining `SILU` and `RELU` separately in the positive and negative domain: these baselines are denoted by `S-R+` and `S-R-`.

	$x < 0$	$x \geq 0$
<code>RELU</code>	0	x
<code>SILU</code>	$x \cdot \sigma(x)$	$x \cdot \sigma(x)$
<code>R-S+</code>	0	$x \cdot \sigma(x)$
<code>S-R+</code>	$x \cdot \sigma(x)$	x

Discussion The stochastic strategy resembles activation dropout (Srivastava et al., 2014), which can be regarded as a particular case of our method where one of the activations is the null function. However, the objective of dropout is to avoid overfitting. Our motivation is closer to Quantization-aware training (Jacob et al., 2017), more specifically, to the QuantNoise strategy of Fan et al. (2020), where the model is pretrained to observe both the train-time (unquantized) and the inference-time (quantized) models. In QuantNoise, using these two modes during training time ensure both the proper optimization, without suffering the flat gradient inherent to quantization, while reducing the discrepancy that results from the late-quantization of the model weights.

Alternative construction of a stochastic activation. An alternative construction is to randomly select between the identity function $x \mapsto x$ and the constant zero function $x \mapsto 0$ with a sigmoidal probability $\sigma(x)$. As a result, in expectation this function is given by

$$\mathbb{E}[\text{sa}(x)] = (1 - \sigma(x)) \cdot 0 + \sigma(x) \cdot x = \sigma(x) \cdot x, \quad (4)$$

where we recognize the `SILU`(x) function. While the simplicity of this construction is mathematically appealing, our preliminary experiments revealed that it does not work very well.

3.3 Inference-time strategies and evaluation

At test time, we evaluate and analyze models trained with `Swi+FT` and/or `StochA` as follows:

RELU at test time This is how we can enable sparsity. The corresponding evaluations therefore measure the performance on benchmarks when using this activation at test time.

Exploiting sparsity On an input $x \in \mathbb{R}^D$, the gated FFN computes:

$$y = W_2 \times (\text{RELU}(W_1 \times x) \odot (W_3 \times x)) \text{ with } W_1, W_3 \in \mathbb{R}^{N \times D} \text{ and } W_2 \in \mathbb{R}^{D \times N}, \quad (5)$$

assuming column vectors and noting \odot the element-wise multiplication. When the activation $\text{RELU}(W_1 \times x)$ has a fraction s of zeros, the multiplications by W_2 and W_3 can exploit this sparsity: the baseline of $3ND$ FLOPS reduces to $(3 - 2s)ND$.

Note that exploiting the sparsity to increase the computational throughput is not straightforward. At training time, the runtime is dominated by matrix-matrix multiplications, where even a 90% sparsity rate is not guaranteed to yield efficiency gains. At inference time with one prompt at a time, the bottleneck is the memory access used during matrix-vector multiplications. When W_2 is stored by rows and W_3 by columns, the sparsity can be exploited to avoid a fraction s of the memory reads, that are contiguous. This implementation nearly yields the expected speedup (see experimental section).

Stochastic activation at test time The following only applies to the `StochA` strategy: we evaluate the performance by leveraging the randomness at test time, i.e., in this case, we do not use `RELU`. This choice is interesting for two reasons:

1. To quantify the effect of the activation discrepancy between train and test.
2. To generate multiple outputs from the same prompt with the randomness of `StochA`.

For the second usage, the standard way to generate multiple outputs from the same prompt is to replace the greedy decoding with a random sampling of the token from its probability distribution. This sampling can be tuned by setting a softmax temperature T which adjusts between completely uniform sampling ($T \rightarrow \infty$) and strict maximum sampling ($T \rightarrow 0$). In both cases, we keep the one generated output with the highest normalized log likelihoods, i.e., the per-token average log-likelihood, as predicted by the model.

4 Experiments with large language models

4.1 Experimental setting

Model architecture We train dense decoder-only models. The transformer blocks use grouped-query attention (Ainslie et al., 2023). These models use RMSNorm (Zhang & Sennrich, 2019) with prenormalization, rotary positional encoding (RoPE) (Su et al., 2021) with $\theta = 500000$ and train with document causal masking. We use the `SILU` activation (Shazeer, 2020) for the `SILU` baseline. The structure of our `LM1.5B` and `LM3B` models is detailed in Table 4 in Appendix A.

Training hyper-parameters We train the models with AdamW optimizer (Loshchilov & Hutter, 2017) with $\beta_1 = 0.9$, $\beta_2 = 0.95$, learning rate of $lr = 3 \times 10^{-3}$, weight decay of 0.1, and gradient clipping at norm 1.0. After 2000 steps of linear warm-up, we use a cosine decay learning rate schedule with peak learning rate 8×10^{-4} and decay by a factor of 1/100 over the training horizon.

Tokenizer We use the Llama3 (Dubey et al., 2024) tokenizer, which is a fast Byte-Pair Encoding tokenizer implemented with TikToken.2 The vocabulary contains 128 000 regular tokens as well as 256 reserved tokens.

Pre-training We pre-train the `LM1.5B` and `LM3B` models with 47B and 80B tokens, respectively, from a diverse collection of mostly English natural language and coding data. We use a batch size of 1M tokens and a context length of 8192 tokens.

Evaluation Benchmarks We employ two types of benchmarks for zero or few-shot evaluation, which we describe in more detail in Appendix G and Table 8. The first type is code generation tasks: HumanEval+ (Liu et al., 2023) and MBPP (Chen et al., 2021). The second type consists of common sense and general reasoning: HellaSWAG (Zellers et al., 2019), ARC (Clark et al., 2018), PIQA (Bisk et al., 2020), OBQA (Mihaylov et al., 2018), WinoGrande (Sakaguchi et al., 2020), NQ (Kwiatkowski et al., 2019), RACE (Lai et al., 2017), TQA (Joshi et al., 2017) and GSM8K (Cobbe et al., 2021).

Activation	Training activation					LM1.5B			LM3B		
	$x < 0$		$x > 0$	p	Swi+FT	train	val	val	train	val	val
	p	$1 - p$		RELU		StochA		RELU	StochA		
SILU	SILU	SILU	-	✗	2.105	2.122*		1.966	1.974*		
RELU	RELU	RELU	-	✗	2.140	2.161		2.027	2.043		
S-R+	SILU	RELU	-	✗	2.101	2.124*		1.970	1.980*		
R-S+	RELU	SILU	-	✗	2.123	2.151*		2.016	2.033*		
[S R]-R+	SILU	RELU	RELU	0.3	✗	2.120	2.363	2.146	1.993	2.257	2.006
[S R]-R+	SILU	RELU	RELU	0.5	✗	2.120	2.507	2.145	1.990	2.889	1.999
[S R]-S+	SILU	RELU	SILU	0.3	✗	2.115	2.305	2.143	1.987	2.257	1.996
[S R]-S+	SILU	RELU	SILU	0.5	✗	2.115	2.530	2.143	1.984	2.753	1.995
[S R]-R+	SILU	RELU	RELU	0.3	✓	2.123	2.141	2.251	1.988	1.998	2.177
[S R]-R+	SILU	RELU	RELU	0.5	✓	2.129	2.148	2.307	1.989	2.002	2.306
[S R]-S+	SILU	RELU	SILU	0.3	✓	2.120	2.138	2.221	1.982	1.992	2.103
[S R]-S+	SILU	RELU	SILU	0.5	✓	2.125	2.144	2.301	1.985	1.994	2.234

Table 1 The train loss is computed over the last 500 steps of the training of LM1.5B, the val loss is measured after training, on a different set of text and code, using the RELU activation* or StochA, i.e. the same activation used at train time (possibly deterministic). If Swi+FT is enabled, we switch to RELU for the last 5% steps. *: for the deterministic baselines SILU, S-R+ and S-R-, we do the inference with the same activation used at train-time (not RELU).

4.2 Performance analysis of Swi+FT and StochA with RELU at inference time

In this section we analyze the effect of our proposal when using RELU at test time. In Appendix B, we provide a complementary analysis of the sparsity. Depending on the setting, the average rate of 0s can be higher than 90%, when using the RELU at test time.

Cross-entropy performance Table 1 summarizes the impact on the training and validation losses of multiple choices with the LM1.5B and LM3B models. We observe that the training loss using stochastic activation at train time is lower than that obtained with RELU. However the validation entropy is not competitive per se, due to the remaining train-inference discrepancy of activation. This is solved by Swi+FT: switching to the RELU activation function and fine-tuning for the last 5% or 10% steps of the training steps drastically boosts the test-time inference. These results outperform the results obtained with regular RELU training, while using the same activation at test time.

Fast inference with RELU sparsity The activation sparsity can be exploited to avoid fetching 90% of the matrices W_1 and W_3 of the FFN (see Eq. 5 and detailed sparsity rates in Appendix B). As a consequence, we observe a direct benefit on CPU: Figure 3 shows that 90% sparsity directly translates into a 65% speedup. On GPU, the speedup of FFN inference is around $1.5\times$. However, because the inference is much faster, different overheads dominate raw computation time of the FFN layers. These include the KV-cache management, Python interpretation, attention masks and Rope management, etc. We expect these overheads to be less significant on larger models.

Absence of dead neurons with Swi+FT Figure 7(left) shows a sudden jump in the RELU CDF, which indicates there are many activations that are exactly zero on input of RELU. The RELU plot in Figure 7(right) shows that a large fraction of the rows of the linear layer W_1 (Eq 5) are near zero (i.e. their norm is less than $1/1000$ the average row norm of the matrix). This means that these rows are unused: they are “dead neurons”. In contrast, the Swi+FT plot in Figure 7(right) we observe that using SILU at pre-training prevents these dead neurons appearing. This explains why our approach obtains significantly better results with RELU than the vanilla training of the model using the RELU from scratch.

Complementarity between StochA and Swi+FT when fine-tuned with RELU Figure 4 shows the training loss when using StochA and Swi+FT jointly. When switching the activation to RELU, we observe a spike in the loss, but the optimization rapidly recovers, and converges to a model that has better performance than

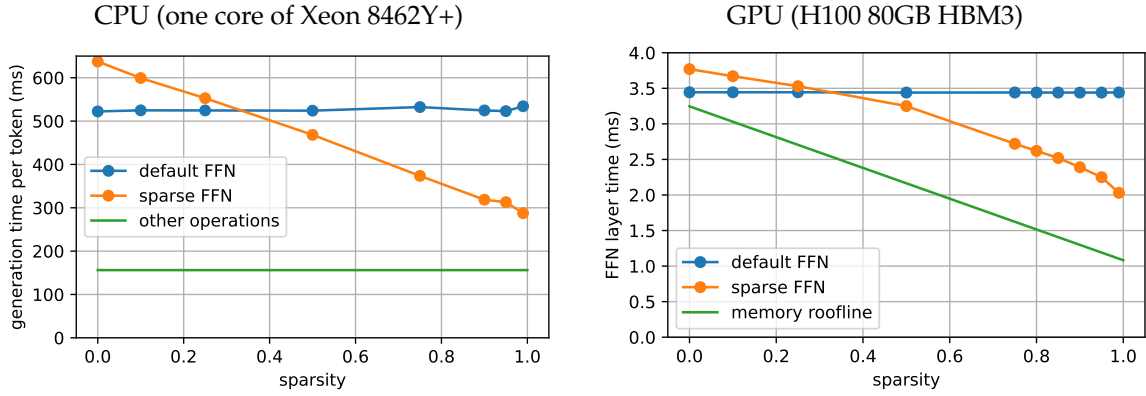


Figure 3 Inference times for 1 token, as a function of the activation sparsity, with a LM3B model trained with *Swi+FT*. For the CPU we indicate the total inference time, including “other operations”: the attention layers (these are not dominant because the generation is limited to 200 tokens), the normalization and the execution overheads. At 90% sparsity the speedup is $\times 1.65$. For the GPU, we measure only the FFN inference time. Note that the impact on inference is less important because at this speed and model scale the overheads are dominant. We also indicate the minimum runtime that could be obtained given the GPU’s memory bandwidth (roofline model).

the one trained with RELU from scratch. In contrast, in the case where we employ *Swi+FT* alone (Figure 2), fine-tuning with RELU after pretraining with SILU is not enough to obtain performance improvements. As a consequence, the *StochA* and *Swi+FT* approaches are complementary.

Impact of fine-tuning with RELU for the last $\alpha * 100\%$ steps In Figure 4, we compare the final loss reported for different values of α . In that case, setting $\alpha = 0.1$ is a good trade-off since the corresponding loss is lower than the RELU loss.

Continuous pre-training with *StochA* and *Swi+FT* Starting from a pre-trained LM1.5B model with SILU, we can leverage either *StochA* or *Swi+FT* methods for continuous pretraining (CPT), see Appendix E for experimental details. In such case, the best strategy is to use *Swi+FT*, i.e., simply fine-tune with RELU the model initially trained with SILU to obtain the best trade-off between sparsity and loss (Table 6). This pattern is the opposite of what we observe for LMs trained from scratch, where the *StochA* and *StochA +Swi+FT* offer the best trade-off between sparsity and loss (Table 1).

Generalizability of *StochA* and *Swi+FT* for any pair of activations In Appendix F, we explain how our methods can be generalized for any pair of activation functions and include an illustrative example with the (TANH,RELU) activations.

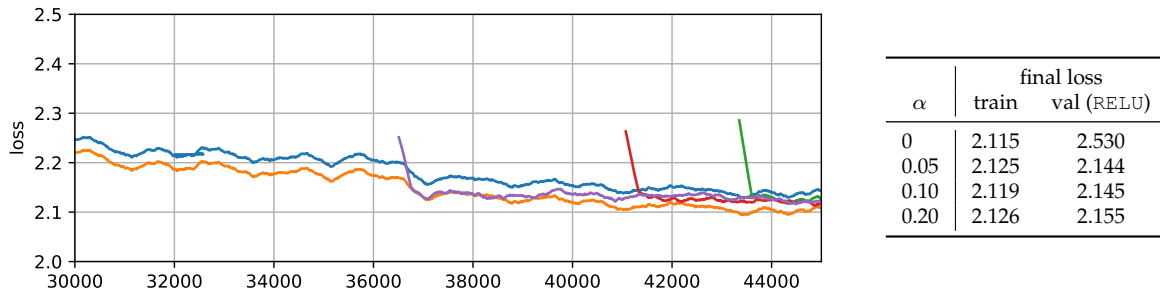


Figure 4 Training loss with *Swi+FT* and *StochA*: [S|R]-S+ activation with $p = 0.5$ for $\alpha * 100\% = 5\%$, 10% and 20% , relative to RELU and SILU. This shows that the *Swi+FT* strategy needs to be combined with *StochA* to provide good models operating with RELU compared to finetuning SILU with RELU alone (Figure 2). This plot this is zoomed in relative to Figure 2.

↓ Benchmark/metric	LM1.5B				LM3B			
	(a) baselines		(b) Swi+FT	(c) StochA	(a) baselines		(b) Swi+FT	(c) StochA
	train activation →	SILU	RELU	[S R]-S+	[S R]-S+	SILU	RELU	[S R]-S+
inference activation →	SILU	RELU	RELU	[S R]-S+	SILU	RELU	RELU	[S R]-S+
hellaswag/acc_char	0.585	0.561	0.574	0.576	0.684	0.633	0.671	0.678
winogrande/acc_char	0.593	0.571	0.568	0.568	0.657	0.615	0.630	0.620
arc_easy/acc_char	0.568	0.562	0.600	0.562	0.675	0.642	0.679	0.671
arc_challenge/acc_char	0.313	0.286	0.331	0.314	0.390	0.348	0.396	0.376
piqa/acc_char	0.732	0.720	0.724	0.720	0.767	0.751	0.765	0.761
obqa/acc_char	0.346	0.340	0.378	0.340	0.390	0.380	0.384	0.408
race.middle/acc_char	0.518	0.516	0.509	0.498	0.565	0.538	0.559	0.549
race.high/acc_char	0.382	0.379	0.372	0.375	0.414	0.402	0.407	0.416
human_eval_plus/pass@1	0.073	0.067	0.049	0.055	0.128	0.110	0.128	0.116
mbpp/compsiles@1	0.978	0.970	0.960	0.980	0.992	0.980	0.990	0.982
tqa/f1	0.243	0.217	0.229	0.232	0.351	0.293	0.327	0.342
nq/f1	0.123	0.107	0.121	0.113	0.169	0.146	0.170	0.145
average performance	0.454	0.441	<u>0.451</u>	0.444	0.515	0.486	<u>0.509</u>	0.505

Table 2 Performance per benchmark of (a) RELU and SILU baselines for LM1.5B and LM3B compared to (b) models with StochA +Swi+FT at train time and RELU at test time, and (c) models with StochA at train and test time. We use the model with the best perplexity on val namely $p = 0.3, \alpha = 0.05$ for Swi+FT and $p = 0.5$ for StochA. The average performance for the topline (SILU) is in bold, second best (StochA +Swi+FT) is underlined.

4.3 Performance on downstream tasks

Detailed results per benchmark Table 2 reports the results for standard code generation, common sense and general reasoning benchmarks detailed in Appendix G. We consider multiple StochA models using few-shot or zero shot prompting, see Table 8 in Appendix G for more details. The model with SILU (topline) is significantly better than a regular model with RELU. However, our models trained with StochA are slightly better or on par with SILU: either the model fine-tuned with Swi+FT and using RELU at inference time, or even the model that uses StochA at test time.

Performance when varying α with Swi+FT Figure 5 shows that we can slightly surpass the SILU baseline average performance if we first use a stochastic activation function during the LM1.5B model training and then switch to the RELU activation for the last $\alpha * 100\%$ of the training steps, for $\alpha \in \{0.05, 0.1, 0.2\}$. The best performance is obtained with $\alpha = 0.05$ or $\alpha = 0.1$ for the LM1.5B model.

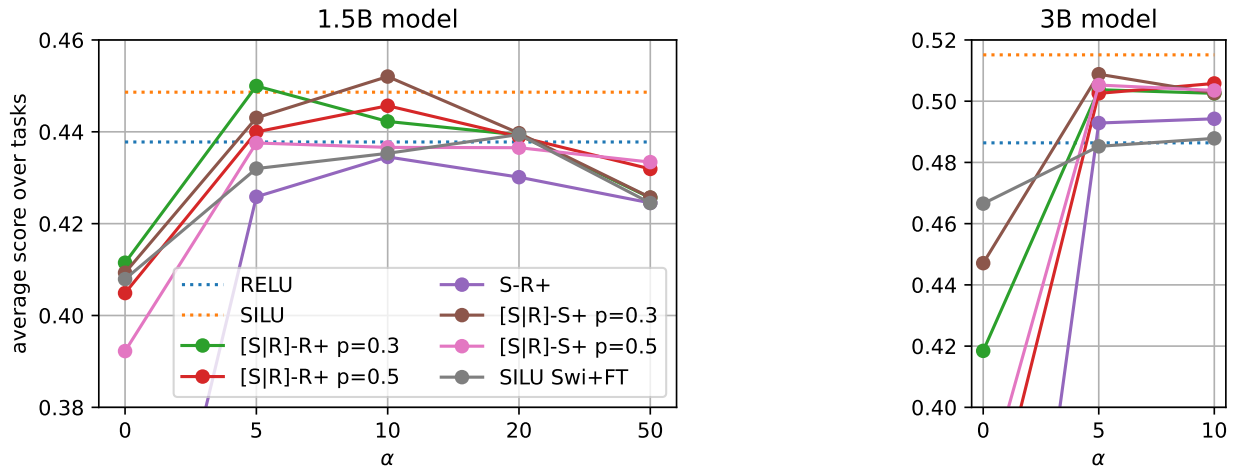


Figure 5 Swi+FT: analysis of the fine-tuning rate α . Average performance over the benchmarks as a function of the percentage α of steps for which we switch to the RELU activation at the end of training. We use RELU at inference time.

p	LM1.5B	LM3B
0 (R-S+)	0.215	0.222
0.3	0.443	0.504
0.5	0.426	0.505
0.7	0.453	0.495
1.0 (SILU)	0.454	0.515

Table 3 *StochA*: Impact on benchmarks performance (avg) as a function of the *StochA* p for [S|R]-S+ used at test time. The case $p = 0$ corresponds to R-S+ while $p = 1$ corresponds to the baseline SILU. The performance increases with more SILU in the mix. However, the stochasticity can be used to increase the generation diversity.

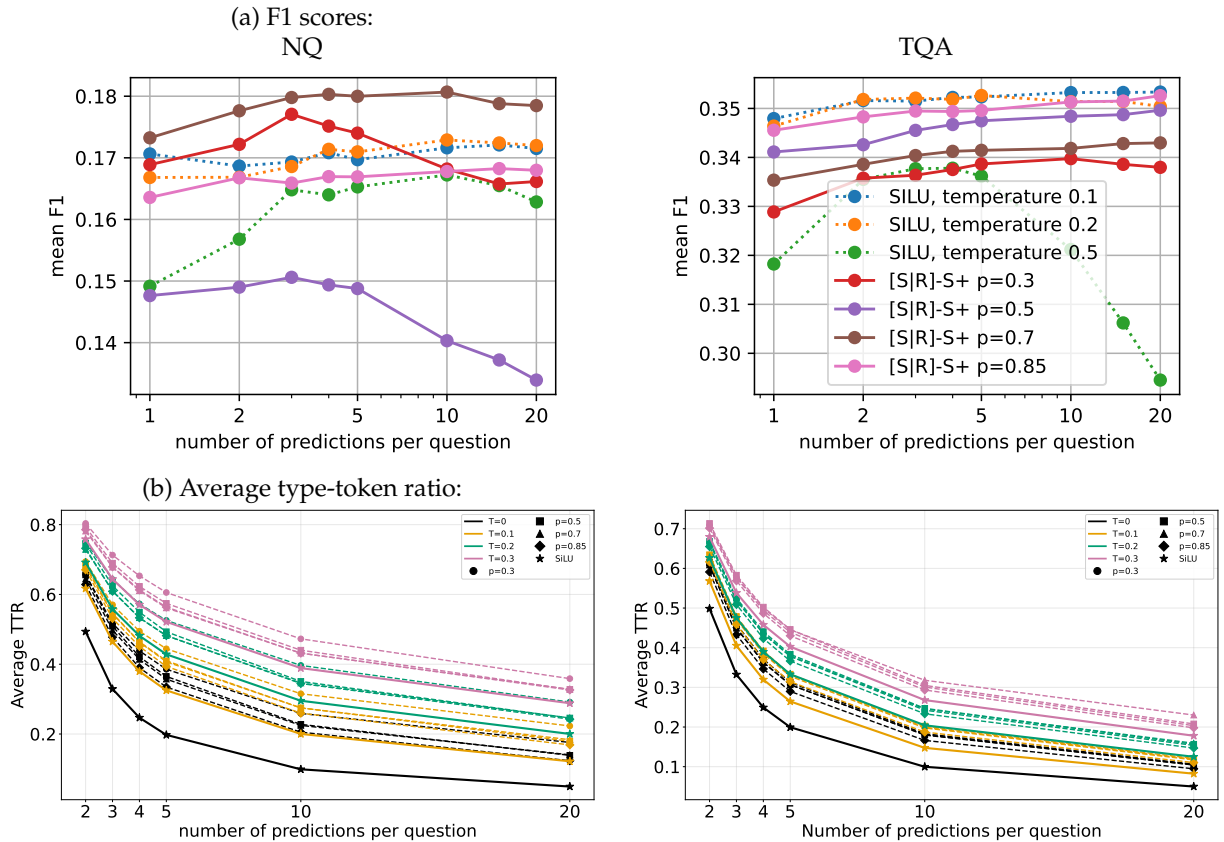


Figure 6 Comparison of diverse response generation methods in Q&A benchmarks. (a) F1 scores when varying the temperature with SILU or [S|R]-S+ p with $\text{temp}=0$, the generations are scored by normalized log likelihoods. (b) TTR when varying the temperature in temperature sampling with SILU (solid lines) vs [S|R]-S+ for different values of p (dashed lines).

4.4 Exploiting *StochA* at test time

Effectiveness of *StochA* at test time In Table 1, in addition to the results with RELU at test time, we also report the train and validation losses obtained when employing *StochA* at test time. We observe that (1) using stochastic activations for inference works surprisingly well in spite of the randomness. The results are between RELU and SILU in most configurations; (2) When using *StochA* at test time, there is no need to fine-tune the model with Swi+FT . This is expected since this strategy is intended to decrease the discrepancy with the test-time activation choice. Table 3 shows that the average benchmark performance generally increases when the stochastic mix approaches SILU. Therefore, *StochA* is primarily useful as a way to generate multiple outputs for the same prompt.

Diversity of generated sequences ablation Figure 6 shows that leveraging the *StochA* activations stochasticity (combined with standard temperature sampling) generates more diverse sequences compared to using

SILU with standard temperature sampling. See Appendix C for the experimental setup and Appendix H for qualitative examples of such generations.

In Figure 6 (a), the curves are increasing, which means that (1) we obtain diverse generations and (2) that the normalized log-likelihood is a suitable scoring function. Specifically, for the NQ task, the StochA activation with $p = 0.7$ and temperature zero yields consistently higher performance than standard temperature sampling with the SILU activation (for temperatures in $\{0.1, 0.2, 0.5\}$). The StochA activation with $p = 0.3$ is also competitive for the number of generations up to five. In contrast, the results are subpar for the TQA task: standard temperature sampling with SILU activation yields higher performances for all number of generations for temperatures in $\{0.1, 0.2\}$.

In Figure 6 (b), we observe that all the models that use StochA activation functions have consistently higher average TTR for both tasks, for each temperature in $\{0, 0.1, 0.2, 0.3\}$ compared to standard temperature sampling with SILU. This finding further confirms that the text diversity of generations is much better for these models.

Token-level diversity ablation In Appendix D, we highlight that using StochA at inference time is equivalent to applying Monte Carlo dropout (Gal & Ghahramani, 2016) on the negative side of the input after activation. We then leverage this token level diversity at inference time by doing multiple forward passes per generated token using greedy decoding. As observed in the sequence level ablation, more diverse tokens are generated. However, we did not observe that this resulted in better performance if the maximum probability or majority vote selection strategies were used.

5 Conclusion

This paper introduces a novel stochastic activation that preserves the performance of a non-sparse activation, such as SILU, while better adjusting to the behavior of a sparse one, such as RELU, at test time. This improves the inference times for the FFN layers of a transformer, translating into a speedup of typically $\times 1.65$ for the FFN processing on CPUs while almost preserving the accuracy of the non-sparse SILU activation. Finally, we explore how stochastic activations can be leveraged at test time to improve diversity in model generations.

References

- Joshua Ainslie, James Lee-Thorp, Michiel de Jong, Yury Zemlyanskiy, Federico Lebron, and Sumit Sanghai. GQA: Training generalized multi-query transformer models from multi-head checkpoints. In Houda Bouamor, Juan Pino, and Kalika Bali (eds.), *Proceedings of the 2023 Conference on Empirical Methods in Natural Language Processing*, pp. 4895–4901, Singapore, December 2023. Association for Computational Linguistics. doi: 10.18653/v1/2023.emnlp-main.298. URL <https://aclanthology.org/2023.emnlp-main.298/>.
- Jacob Austin, Augustus Odena, Maxwell Nye, Maarten Bosma, Henryk Michalewski, David Dohan, Ellen Jiang, Carrie J. Cai, Michael Terry, Quoc V. Le, and Charles Sutton. Program synthesis with large language models. *ArXiv*, abs/2108.07732, 2021. URL <https://api.semanticscholar.org/CorpusID:237142385>.
- Hangbo Bao, Li Dong, and Furu Wei. Beit: Bert pre-training of image transformers. *ArXiv*, abs/2106.08254, 2021. URL <https://api.semanticscholar.org/CorpusID:235436185>.
- Yoshua Bengio, Nicholas Léonard, and Aaron C. Courville. Estimating or propagating gradients through stochastic neurons for conditional computation. *ArXiv*, abs/1308.3432, 2013. URL <https://api.semanticscholar.org/CorpusID:18406556>.
- Yonatan Bisk, Rowan Zellers, Ronan Le bras, Jianfeng Gao, and Yejin Choi. Piqa: Reasoning about physical commonsense in natural language. *Proceedings of the AAAI Conference on Artificial Intelligence*, 34(05):7432–7439, Apr. 2020. doi: 10.1609/aaai.v34i05.6239. URL <https://ojs.aaai.org/index.php/AAAI/article/view/6239>.
- Tom B Brown, Benjamin Mann, Nick Ryder, Melanie Subbiah, Jared Kaplan, Prafulla Dhariwal, Arvind Neelakantan, Pranav Shyam, Girish Sastry, Amanda Askell, et al. Language models are few-shot learners. *arXiv preprint arXiv:2005.14165*, 2020.

- Mark Chen, Jerry Tworek, Heewoo Jun, Qiming Yuan, Henrique Ponde de Oliveira Pinto, Jared Kaplan, and OpenAI team. Evaluating large language models trained on code. 2021.
- Aakanksha Chowdhery, Sharan Narang, Jacob Devlin, and Google team. Palm: Scaling language modeling with pathways, 2022. URL <https://arxiv.org/abs/2204.02311>.
- Peter Clark, Isaac Cowhey, Oren Etzioni, Tushar Khot, Ashish Sabharwal, Carissa Schoenick, and Oyvind Tafjord. Think you have solved question answering? try arc, the ai2 reasoning challenge. *ArXiv*, abs/1803.05457, 2018. URL <https://api.semanticscholar.org/CorpusID:3922816>.
- Karl Cobbe, Vineet Kosaraju, Mo Bavarian, Mark Chen, Heewoo Jun, Lukasz Kaiser, Matthias Plappert, Jerry Tworek, Jacob Hilton, Reiichiro Nakano, Christopher Hesse, and John Schulman. Training verifiers to solve math word problems. *ArXiv*, abs/2110.14168, 2021. URL <https://api.semanticscholar.org/CorpusID:239998651>.
- DeepSeek-AI, Aixin Liu, Bei Feng, Bin Wang, Bingxuan Wang, Bo Liu, Chenggang Zhao, Chengqi Deng, Chong Ruan, Damai Dai, Daya Guo, et al. Deepseek-v2: A strong, economical, and efficient mixture-of-experts language model, 2024. URL <https://arxiv.org/abs/2405.04434>.
- Jacob Devlin, Ming-Wei Chang, Kenton Lee, and Kristina Toutanova. Bert: Pre-training of deep bidirectional transformers for language understanding, 2019. URL <https://arxiv.org/abs/1810.04805>.
- Abhimanyu Dubey, Abhinav Jauhri, Abhinav Pandey, Abhishek Kadian, Ahmad Al-Dahle, Aiesha Letman, Akhil Mathur, Alan Schelten, Amy Yang, Angela Fan, et al. The llama 3 herd of models, 2024. URL <https://arxiv.org/abs/2407.21783>.
- Angela Fan, Edouard Grave, and Armand Joulin. Reducing transformer depth on demand with structured dropout. *arXiv preprint arXiv:1909.11556*, 2019.
- Angela Fan, Pierre Stock, Benjamin Graham, Edouard Grave, Rémi Gribonval, Herve Jegou, and Armand Joulin. Training with quantization noise for extreme model compression. *arXiv preprint arXiv:2004.07320*, 2020.
- Yarin Gal and Zoubin Ghahramani. Dropout as a bayesian approximation: representing model uncertainty in deep learning. In *Proceedings of the 33rd International Conference on International Conference on Machine Learning - Volume 48*, ICML'16, pp. 1050–1059. JMLR.org, 2016.
- Golnaz Ghiasi, Tsung-Yi Lin, and Quoc V. Le. Dropblock: A regularization method for convolutional networks, 2018. URL <https://arxiv.org/abs/1810.12890>.
- Xavier Glorot, Antoine Bordes, and Yoshua Bengio. Deep sparse rectifier neural networks. In *Proceedings of the fourteenth international conference on artificial intelligence and statistics*, pp. 315–323. JMLR Workshop and Conference Proceedings, 2011.
- Yinglong Guo, Shaohan Li, and Gilad Lerman. The effect of leaky relus on the training and generalization of overparameterized networks. *CoRR*, abs/2402.11942, 2024. doi: 10.48550/ARXIV.2402.11942. URL <https://doi.org/10.48550/arXiv.2402.11942>.
- Kaiming He, Xinlei Chen, Saining Xie, Yanghao Li, Piotr Dollár, and Ross Girshick. Masked autoencoders are scalable vision learners. In *2022 IEEE/CVF Conference on Computer Vision and Pattern Recognition (CVPR)*, pp. 15979–15988, 2022. doi: 10.1109/CVPR52688.2022.01553.
- Dan Hendrycks and Kevin Gimpel. Gaussian error linear units (gelus). *arXiv: Learning*, 2016. URL <https://api.semanticscholar.org/CorpusID:125617073>.
- Geoffrey Hinton. Neural networks for machine learning. Coursera, video lectures, 2012. Online course.
- Benoit Jacob, Skirmantas Kligys, Bo Chen, Menglong Zhu, Matthew Tang, Andrew G. Howard, Hartwig Adam, and Dmitry Kalenichenko. Quantization and training of neural networks for efficient integer-arithmetical-only inference. *2018 IEEE/CVF Conference on Computer Vision and Pattern Recognition*, pp. 2704–2713, 2017. URL <https://api.semanticscholar.org/CorpusID:39867659>.
- Albert Q. Jiang, Alexandre Sablayrolles, Antoine Roux, Arthur Mensch, Blanche Savary, Chris Bamford, Devendra Singh Chaplot, Diego de Las Casas, Emma Bou Hanna, Florian Bressand, Gianna Lengyel, Guillaume Bour, Guillaume Lample, Léo Renard Lavaud, Lucile Saulnier, Marie-Anne Lachaux, Pierre Stock, Sandeep Subramanian, Sophia Yang, Szymon Antoniak, Teven Le Scao, Théophile Gervet, Thibaut Lavril, Thomas Wang, Timothée Lacroix, and William El Sayed. Mixtral of experts. *ArXiv*, abs/2401.04088, 2024. URL <https://api.semanticscholar.org/CorpusID:266844877>.

- as editor Johnson, Wendell. Studies in language behavior: A program of research. *Psychological Monographs*, 56(2):1–15, 1944.
- Mandar Joshi, Eunsol Choi, Daniel Weld, and Luke Zettlemoyer. Triviaqa: A large scale distantly supervised challenge dataset for reading comprehension. 05 2017. doi: 10.48550/arXiv.1705.03551.
- Herve Jégou, Matthijs Douze, and Cordelia Schmid. Product quantization for nearest neighbor search. *IEEE Transactions on Pattern Analysis and Machine Intelligence*, 33(1):117–128, 2011. doi: 10.1109/TPAMI.2010.57.
- Günter Klambauer, Thomas Unterthiner, Andreas Mayr, and Sepp Hochreiter. Self-normalizing neural networks. In *Neural Information Processing Systems*, 2017. URL <https://api.semanticscholar.org/CorpusID:13713980>.
- Tom Kwiatkowski, Jennimaria Palomaki, Olivia Redfield, Michael Collins, Ankur Parikh, Chris Alberti, Danielle Epstein, Illia Polosukhin, Jacob Devlin, Kenton Lee, Kristina Toutanova, Llion Jones, Matthew Kelcey, Ming-Wei Chang, Andrew M. Dai, Jakob Uszkoreit, Quoc Le, and Slav Petrov. Natural questions: A benchmark for question answering research. *Transactions of the Association for Computational Linguistics*, 7:452–466, 2019. doi: 10.1162/tacl_a_00276. URL <https://aclanthology.org/Q19-1026>.
- Guokun Lai, Qizhe Xie, Hanxiao Liu, Yiming Yang, and Eduard H. Hovy. Race: Large-scale reading comprehension dataset from examinations. In *Conference on Empirical Methods in Natural Language Processing*, 2017. URL <https://api.semanticscholar.org/CorpusID:6826032>.
- Guillaume Lample, Alexandre Sablayrolles, Marc’Aurelio Ranzato, Ludovic Denoyer, and Hervé Jégou. Large memory layers with product keys. *Advances in Neural Information Processing Systems*, 32, 2019.
- Kyungsu Lee, Jaeseung Yang, Haeyun Lee, and Jae Youn Hwang. Stochastic adaptive activation function. In *Proceedings of the 36th International Conference on Neural Information Processing Systems, NIPS ’22*, Red Hook, NY, USA, 2022. Curran Associates Inc. ISBN 9781713871088.
- Jiawei Liu, Chunqiu Steven Xia, Yuyao Wang, and Lingming Zhang. Is your code generated by chatGPT really correct? rigorous evaluation of large language models for code generation. In *Thirty-seventh Conference on Neural Information Processing Systems*, 2023. URL <https://openreview.net/forum?id=lqvx610Cu7>.
- Ilya Loshchilov and Frank Hutter. Decoupled weight decay regularization. In *International Conference on Learning Representations*, 2017. URL <https://api.semanticscholar.org/CorpusID:53592270>.
- Andrew L Maas, Awni Y Hannun, Andrew Y Ng, et al. Rectifier nonlinearities improve neural network acoustic models. In *Proc. icml*, volume 30, pp. 3. Atlanta, GA, 2013.
- Todor Mihaylov, Peter Clark, Tushar Khot, and Ashish Sabharwal. Can a suit of armor conduct electricity? a new dataset for open book question answering. In Ellen Riloff, David Chiang, Julia Hockenmaier, and Jun’ichi Tsujii (eds.), *Proceedings of the 2018 Conference on Empirical Methods in Natural Language Processing*, pp. 2381–2391, Brussels, Belgium, October–November 2018. Association for Computational Linguistics. doi: 10.18653/v1/D18-1260. URL <https://aclanthology.org/D18-1260/>.
- Siyuan Mu and Sen Lin. A comprehensive survey of mixture-of-experts: Algorithms, theory, and applications, 03 2025.
- Prajit Ramachandran, Barret Zoph, and Quoc V. Le. Searching for activation functions. *ArXiv*, abs/1710.05941, 2018. URL <https://api.semanticscholar.org/CorpusID:10919244>.
- Joseph Redmon, Santosh Kumar Divvala, Ross B. Girshick, and Ali Farhadi. You only look once: Unified, real-time object detection. *2016 IEEE Conference on Computer Vision and Pattern Recognition (CVPR)*, pp. 779–788, 2015. URL <https://api.semanticscholar.org/CorpusID:206594738>.
- Tal Ridnik, Hussam Lawen, Asaf Noy, Emanuel Ben, Baruch Gilad Sharir, and Itamar Friedman. Tresnet: High performance gpu-dedicated architecture. In *2021 IEEE Winter Conference on Applications of Computer Vision (WACV)*, pp. 1399–1408, 2021. doi: 10.1109/WACV48630.2021.00144.
- Keisuke Sakaguchi, Ronan Le Bras, Chandra Bhagavatula, and Yejin Choi. Winogrande: An adversarial winograd schema challenge at scale. *Proceedings of the AAAI Conference on Artificial Intelligence*, 34(05):8732–8740, Apr. 2020. doi: 10.1609/aaai.v34i05.6399. URL <https://ojs.aaai.org/index.php/AAAI/article/view/6399>.
- Noam M. Shazeer. Glu variants improve transformer. *ArXiv*, abs/2002.05202, 2020. URL <https://api.semanticscholar.org/CorpusID:211096588>.
- Nitish Srivastava, Geoffrey Hinton, Alex Krizhevsky, Ilya Sutskever, and Ruslan Salakhutdinov. Dropout: a simple way to prevent neural networks from overfitting. *The journal of machine learning research*, 15(1):1929–1958, 2014.

- Jianlin Su, Yu Lu, Shengfeng Pan, Bo Wen, and Yunfeng Liu. Roformer: Enhanced transformer with rotary position embedding. *ArXiv*, abs/2104.09864, 2021. URL <https://api.semanticscholar.org/CorpusID:233307138>.
- Hugo Touvron, Thibaut Lavril, Gautier Izacard, Xavier Martinet, Marie-Anne Lachaux, Timothée Lacroix, Baptiste Rozière, Naman Goyal, Eric Hambro, Faisal Azhar, Aurélien Rodriguez, Armand Joulin, Edouard Grave, and Guillaume Lample. Llama: Open and efficient foundation language models. *ArXiv*, abs/2302.13971, 2023. URL <https://api.semanticscholar.org/CorpusID:257219404>.
- Ashish Vaswani, Noam M. Shazeer, Niki Parmar, Jakob Uszkoreit, Llion Jones, Aidan N. Gomez, Lukasz Kaiser, and Illia Polosukhin. Attention is all you need. In *Neural Information Processing Systems*, 2017. URL <https://api.semanticscholar.org/CorpusID:13756489>.
- Tianwen Wei, Bo Zhu, Liang Zhao, Cheng Cheng, Biye Li, Weiwei Lü, Peng Cheng, Jianhao Zhang, Xiaoyu Zhang, Liang Zeng, Xiaokun Wang, Yutuan Ma, Rui Hu, Shuicheng Yan, Han Fang, and Yahui Zhou. Skywork-moe: A deep dive into training techniques for mixture-of-experts language models, 2024. URL <https://arxiv.org/abs/2406.06563>.
- Qwen An Yang, Baosong Yang, Beichen Zhang, Binyuan Hui, Bo Zheng, Bowen Yu, Chengyuan Li, Dayiheng Liu, Fei Huang, Guanting Dong, Haoran Wei, Huan Lin, Jian Yang, Jianhong Tu, Jianwei Zhang, Jianxin Yang, Jiaxin Yang, Jingren Zhou, Junyang Lin, Kai Dang, Keming Lu, Keqin Bao, Kexin Yang, Le Yu, Mei Li, Mingfeng Xue, Pei Zhang, Qin Zhu, Rui Men, Runji Lin, Tianhao Li, Tingyu Xia, Xingzhang Ren, Xuancheng Ren, Yang Fan, Yang Su, Yi-Chao Zhang, Yuyang Wan, Yuqi Liu, Zeyu Cui, Zhenru Zhang, Zihan Qiu, Shanghaoran Quan, and Zekun Wang. Qwen2.5 technical report. *ArXiv*, abs/2412.15115, 2024. URL <https://api.semanticscholar.org/CorpusID:274859421>.
- Rowan Zellers, Ari Holtzman, Yonatan Bisk, Ali Farhadi, and Yejin Choi. Hellaswag: Can a machine really finish your sentence? In *Annual Meeting of the Association for Computational Linguistics*, 2019. URL <https://api.semanticscholar.org/CorpusID:159041722>.
- Biao Zhang and Rico Sennrich. Root mean square layer normalization. *ArXiv*, abs/1910.07467, 2019. URL <https://api.semanticscholar.org/CorpusID:113405151>.

APPENDIX

In this appendix, we add some extra details to complement the main paper. Appendix A gives architectural details for the models used in the paper. Appendix B gives additional details of the sparsity produced by the models that use the `StochA` and `Swi+FT` activations. Appendix C provides the experimental details for the diversity of generations ablation. Appendix D provides the experimental details for the multiple forward passes per generated token ablation. Appendix E gives some details for the CPT experiment with `StochA` and `Swi+FT`. Appendix F discusses how to generalize the `StochA` and `Swi+FT` methods for any pair of non-sparse and sparse activations. Appendix G gives the references for all the benchmarks used in the experiments. The final Appendix H gives some examples of multiple answers generated by `StochA`.

A Architecture detail

The model architectures we use in the paper are loosely inspired by Llama 3. Table 4 summarizes their main parameters.

Parameter	LM1.5B	LM3B
Number of parameters	1.5B	3B
Layers	28	36
Hidden dimension	1536	2048
Intermediate dimension	8960	11008
Number of attention heads	12	16
Number of key-value heads	2	2

Table 4 LM1.5B and LM3B model parameters

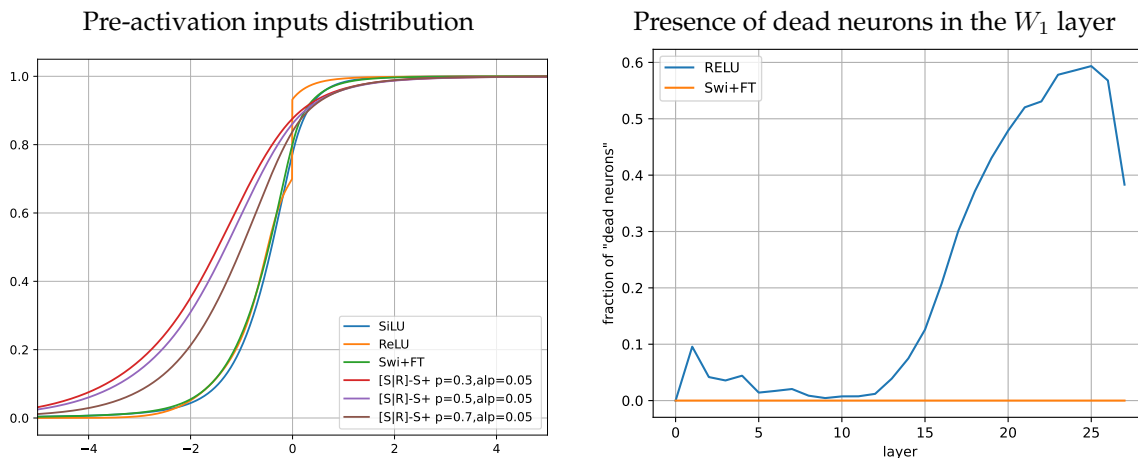


Figure 7 *Left*: empirical cumulative distribution functions for the inputs to the activation functions when training the LM1.5B model with one of the following activations: SILU, ReLU, Swi+FT fine-tuning and the combination of StochA with Swi+FT for different values of p . *Right*: fraction of near-zero rows of the W_1 matrix, indicating useless neurons for two types of activations.

B Sparsity Analysis

In Table 5, we report the sparsity ratios resulting from the gating in the FFN layer, when using the following activations: ReLU, SILU, Swi+FT fine-tuning, and when using StochA with Swi+FT for varying values p . In all cases, except for the SILU baseline, we use ReLU at test time. We observe that Swi+FT fine-tuning with ReLU brings back a lot of sparsity (80%), yet the model is not competitive. The combination of StochA with Swi+FT leads to models offering a high sparsity degree by using ReLU at test time and simultaneously achieving competitive performance, see Tables 1 and 2.

In Figure 7 (*left*), we observe that $P(X \leq 0)$ is the highest for ReLU since most of its mass is concentrated around zero as in Table 5. For $x < 0$, the probability $P(X \leq x)$ is lower for SILU than for both Swi+FT and when we combine StochA with Swi+FT for different values of p . This shows that combining StochA with Swi+FT enables us to control how much mass we assign to negative values of x depending on p .

C Diversity of generations ablation experimental setup

We use the LM3B models trained with the StochA activation [S|R]-S+ with p in $\{0.3, 0.5, 0.7, 0.85\}$. At inference time, the probability p is set to be the same as the one during training. We generate twenty answers for the NQ and TQA generation tasks, compute the F1 and Type-token ratio (TTR) metrics of n generated answers (samples) and average over all datapoints for a given number of samples n in $\{2, 3, 4, 5, 10, 20\}$.

In Figure 6 (b) we report the type-token ratio metric (Johnson, 1944), a simple and widely used metric in

	train	inference	Swi+FT	StochA: p	Swi+FT: α	sparsity (%)
baselines	SILU	SILU	\times	-		0.0002
	ReLU	ReLU	\times	-		94.8
Swi+FT	SILU	ReLU	\checkmark	-	0.05	79.9
StochA	[S R]-S+	ReLU	\checkmark	0.3	0.05	88.5
+Swi+FT	[S R]-S+	ReLU	\checkmark	0.5	0.05	86.5
	[S R]-S+	ReLU	\checkmark	0.7	0.05	84.6

Table 5 We report the rate of the 0-valued activation after the SILU (not sparse) and ReLU activation, when training with the LM1.5B model with the following activations: ReLU, SILU, Swi+FT fine-tuning, and when using StochA with Swi+FT for varying values of p .

linguistics and natural language processing to measure lexical diversity in a text. In this context, a *type* consists of a unique word in the text and a *token* consists of any word occurrence in the text (including repetitions). The Type-Token Ratio is then $TTR = \text{Number of Types} / \text{Number of Tokens}$.

D Multiple forward passes per generated token

If we use the `StochA` activation function, it is equivalent to doing Monte Carlo dropout (Gal & Ghahramani, 2016) on the negative side of the input after activation: it is set to zero with probability $1 - p$. For this reason, at test time, if we run multiple forward passes, this naturally creates a random output after activation which is either zero or `SILU` on the negative side of the inputs after activation.

In this setup, at generation time, after performing the multiple forward passes, we select the next token according to the following strategies:

Max probability: we select the token that has the highest probability.

Majority vote: we select the next token based on the token which appears the most often across the multiple passes.

Results. We use `LM3B` models trained with the `[S|R]-S+` activations with p in $\{0.3, 0.5, 0.7, 0.85\}$. We vary the number of forward passes in $\{5, 10, 15, 20, 30\}$. We report the average performance of the generation tasks `nq`, `tqa`, `mbsp` and `human eval` plus and greedy decoding. Our findings indicate that even though we observe more diversity at the token level, the majority vote and maximum probability strategies do not perform better than the baseline, where we have a single forward pass as we increase the number of forward passes.

E Continuous Pretraining LM1.5B models

We can leverage the `StochA` and `Swi+FT` methods for continuous pretraining (CPT) language models, besides using these activations to train LMs from scratch. In this experiment, we start from the `LM1.5B` models pretrained with the `SILU` activation. During CPT, we use i) `Swi+FT` ii) `StochA` with $p = 0.3$ or $p = 0.5$ or iii) `StochA` and `Swi+FT` with $p = 0.5$ and $\alpha = 0.1$. We use the same number of steps used in the pretraining experiments: 45,629 steps. We compare the training losses against the baseline model that keeps `SILU` during CPT.

	pretrain	CPT	inference	StochA: p	sparsity (%)	train loss
baseline	SILU	SILU	SILU	-	0.0002	2.076
Swi+FT	SILU	RELU	RELU	-	90.96	<u>2.086</u>
StochA	SILU	StochA	RELU	0.5	41.02	2.095
	SILU	StochA	RELU	0.3	57.93	2.095
StochA +Swi+FT	SILU	StochA +Swi+FT	RELU	0.5	<u>81.61</u>	2.096

Table 6 We report the rate of the 0-valued activations and training losses when doing CPT with the `LM1.5B` model with the following activations: `RELU`, `SILU`, `Swi+FT`, `StochA` and when using `StochA` with `Swi+FT` for varying values p .

F StochA and Swi+FT for (TANH, RELU) activations

Our `StochA` and `Swi+FT` methods can be generalized, starting with any pair of non-sparse, sparse activations, in the following way:

1. `StochA`: the non-sparse (activation which takes non-zero values on the negative side) and sparse activation pair can be used as a stochastic activation function that takes the form of either of the

Activation	Training activation					LM1.5B		
	$x < 0$		$x > 0$	p	Swi+FT	train	val	val
	p	$1 - p$				ReLU	StochA	
TANH	TANH	TANH	TANH	-	✗	2.133	2.155	
RELU	RELU	RELU	RELU	-	✗	2.140	2.162	
Tanh+FT	TANH	TANH	TANH	-	✓	2.193	2.224	
[T R]-T+	TANH	RELU	TANH	0.3	✗	2.368	10.803	2.421
[T R]-T+	TANH	RELU	TANH	0.5	✗	2.314	10.997	2.359

Table 7 Losses: train is computed over the last 500 steps of the training loss of LM1.5B, val is measured after training on a different set of text and code using the RELU activation* or StochA, i.e., the same activation used at train time (possibly deterministic). If Swi+FT is enabled, we switch to RELU for the last 10% steps.

activations on the positive side, and, on the negative side, it either takes the non-zero value of the non-sparse variant with probability p or is set to zero with probability $1 - p$.

- Swi+FT: we start with an LM with a non-sparse activation and train it for $(1 - \alpha)\%$ steps. Successively, we finetune the LM with the sparse activation for $\alpha\%$ of the final steps.

To illustrate how the StochA and Swi+FT methods are generalizable, we use the pair of (TANH, RELU) activations. We pretrain a LM1.5B with TANH as the non-sparse activation and RELU as the sparse one for 1) and 2). We compare these versus the losses to the corresponding baselines: using only the TANH or only the RELU activations, respectively. We denote the activation for 1) as Tanh+FT with parameter α and for 2), with [T|R]-T+ with parameter p .

We observe that there is barely any gap between the train loss of the non-sparse (TANH, bolded) and the sparse (RELU, in red) activations, hence, there is no trade-off between sparsity and performance, in contrast to the (SiLU, RELU) case.

G Benchmarks

Code generation We use two benchmarks that evaluate the code generation capabilities of AI models: HumanEval+ and MBPP.

- The HumanEval+ (Liu et al., 2023) benchmark is an extension of HumanEval (Chen et al., 2021), which is designed to evaluate the functional correctness of code generated by AI models.
- MBPP (Austin et al., 2021) is designed to evaluate the code generation abilities of AI models, particularly for Python programming tasks.

Common sense and general reasoning We use benchmarks consisting of question-answer or multiple-choice questions designed to evaluate the commonsense reasoning abilities of AI models, particularly in the context of natural language understanding: HellaSWAG, ARC, PIQA, OBQA, Winogrande, NaturalQuestions, RACE, TQA and GSM8K.

- HellaSWAG (Zellers et al., 2019) consists of multiple-choice questions where each question contains a short context (a sentence or paragraph) followed by four possible continuations. Only one continuation is correct and makes sense given the context.
- The AI Reasoning Challenge (ARC) (Clark et al., 2018) benchmark consists of multiple-choice science questions typically found in elementary and middle school exams. The ARC questions require a mix of factual knowledge, commonsense reasoning, and multi-step inference.
- The Physical Interaction Question-Answering (PIQA) (Bisk et al., 2020) benchmark consists of multiple-choice questions about how to accomplish simple physical tasks. Each question presents a short scenario and two possible solutions; only one is physically plausible.

Benchmark	Metric	Few Shot	Type
hellaswag	acc_char	0	choice
winogrande	acc_char	0	choice
arc_easy	acc_char	0	choice
arc_challenge	acc_char	0	choice
piqa	acc_char	0	choice
obqa	acc_char	0	choice
race.middle	acc_char	0	choice
race.high	acc_char	0	choice
human_eval_plus	pass@1	0	generation
mbpp	compiles@1	3	generation
tqa	f1	5	generation
nq	f1	5	generation

Table 8 Summary of benchmarks used for evaluation. We few-shot prompt the LM1.5B and LM3B models. The metric depends on the benchmark as well as the average performance.

- The OpenBook QA (OBQA) (Mihaylov et al., 2018) benchmark consists of 6,000 multiple-choice questions based on elementary science facts. Each question is designed to require combining a provided “open book” science fact with additional commonsense or general knowledge.
- WinoGrande (Sakaguchi et al., 2020) benchmark consists of multiple-choice questions. Each question presents a sentence with a pronoun and two possible antecedents; the task is to choose the correct referent for the pronoun.
- Natural Questions (NQ) (Kwiatkowski et al., 2019) benchmark is designed to evaluate the ability of an AI model to answer real user questions using information from Wikipedia.
- The Reading Comprehension from Examinations (RACE) (Lai et al., 2017) benchmark consists of passages and multiple-choice questions to assess how well AI models can comprehend and reason about written passages.
- The Trivia QA benchmark (TQA) (Joshi et al., 2017) is a reading comprehension dataset that pairs trivia questions with evidence documents from which answers can be derived.
- The Grade School Math 8k (GSM8k) (Cobbe et al., 2021) benchmark is a dataset of 8,500 high-quality, linguistically diverse grade school math word problems. The benchmark is designed to test multi-step mathematical reasoning capabilities in language models.

H Examples of various sequences generated with StochA

We use a pre-trained LM3B model with StochA, we can use the StochA activation at test time to generate multiple predictions by leveraging the randomness from the activation function. In Table 9, we provide two examples of the generations obtained using questions from the TQA benchmark (Joshi et al., 2017):

question and accepted answers	generated answers	number of times	NLL score	F1 score
When did ibuprofen become available over the counter? A: 1983 A: 1984	1988	4	1.002	0
	1982	11	1.004	0
	1980	1	1.030	0
	1995	2	1.019	0
	2001	1	1.017	0
	1983	1	1.024	1

Continued on next page

Table 9 – Continued from previous page

question and accepted answers	generated answers	number of times	NLL score	F1 score
Who played michael jackson in jackson 5 movie? A:alex burrall A:abolade david olatunde A:wylie draper A:jason weaver	Michael Jackson	19	0.948	0
	Michael jackson	1	0.792	0
Where is the meridian that is opposite the prime meridian located? A:180th meridian A:antimeridian	Greenwich	9	0.896	0
	Greenwich, England	11	0.551	0
The cold dry winds that blow over northern india in winter are called? A:northeast monsoon A:retreating monsoon A:northeast monsoon or retreating monsoon	Siberian	7	1.099	0
	Siberian winds	6	0.970	0
	Ganges	1	1.617	0
	monsoon	2	1.051	2/3
	katabatic winds	3	0.738	0
Where can you find dna in the body? A:chromosomes in cell A:inside cell nucleus	Blood	6	1.262	0
	Hair	12	1.393	0
	Mitochondria	1	0.700	0
	In the nucleus	1	1.437	2/5
Who is often associated with printing the first book using moveable type in germany? A:johannes gutenberg	Johannes Gutenberg	20	0.205	1
Who won the womens 2017 ncaa basketball tournament? A:south carolina	Kentucky	15	1.852	0
	Kentucky Wildcats	1	1.304	0
	North Carolina	4	1.342	1/2
Country with most olympic gold medals all time? A:united states	USA	14	0.818	0
	United States	6	0.614	1
The atomic number of indium which belongs to 5th period is? A:49	5	14	0.579	0
	49	5	0.650	1
	84	1	0.695	0
Who appoints the members of the board of governors of the federal reserve? A:president	The president	16	0.602	1
	The president of the United States	4	0.431	2/5

Continued on next page

Table 9 – Continued from previous page

question and accepted answers	generated answers	number of times	NLL score	F1 score
What age do you need to be to buy a bb gun? A:18		14	0.660	0
		10	0.680	0
		18	0.728	1
What genre is the magic tree house books? A:childrens historical fantasy	Fantasy	14	1.038	1/2
	Children’s fiction	1	1.051	2/5
	Children’s	3	1.245	1/2
	Children’s books	2	1.067	2/5
What is the name of the skin between your nostrils? A:nasal septum A:septum	Nasal septum	17	0.707	1
	Nasion	3	1.224	0

Table 9 Example generations. For each question, we indicate the ground-truth answers (from the dataset). We generate 20 answers per question with $[S|R]_{-S+}$, $p=0.7$. We list the de-duplicated answers, with the NLL score (used to sort the results) and the F1 score (used to evaluate the result, it is computed as the intersection of bags-of-words).